Int. J. Electrochem. Sci., 14 **(2019)** 9030 – 9041, doi: 10.20964/2019.09.75

International Journal of
ELECTROCHEMICAL
SCIENCE
www.electrochemsci.org

An Electrochemical Sensor on the Novel MgO-PEDOT:PSS Platform for Sensitive Bisphenol A Determination

Li Zheng[*], *Yajing Zhu*

College of Chemistry and Chemical Engineering, Xi'an Shiyou University, Xi'an, 710065, PR China
[*]E-mail: lzheng@xsyu.edu.cn

Received: 1 June 2019 / *Accepted:* 10 July 2019 / *Published:* 5 August 2019

A novel magnesium oxide and poly(3,4-ethylenedioxythiophene):poly(styrene-sulfonate) (PEDOT:PSS) composite modified carbon paste electrode (MgO-PP/CPE) has been fabricated for the sensitive quantification of bisphenol A (BPA). The modified electrode was characterized by scanning electron microscopy (SEM), chronocoulometry and electrochemical impedance spectroscopy (EIS). Compared with MgO/CPE, PP/CPE, and CPE, MgO-PP/CPE exhibited enhanced electrochemical activity toward the oxidation of BPA, which was due to the high surface area of MgO and facile electron transfer ability of PEDOT:PSS. Under the optimum conditions, the linear sweep voltammetric oxidation peak current of BPA was linear with its concentration in the ranges from 1.0 nM to 0.4 μM and 0.4 to 10 μM, with a low detection limit of 0.5 nM (3S/N). The fabricated sensor was successively applied to the quantification of BPA content in water samples.

Keywords: Bisphenol A; MgO; PEDOT:PSS; Electrochemical Sensor; Carbon Paste Electrode

1. INTRODUCTION

Bisphenol A (BPA) is an organic monomer, widely used in the production of epoxy resins and polycarbonate plastics for packages and containers [1]. However, BPA is also an endocrine disruptor, which can interfere with the human body's hormonal activities, increase the risk of heart disease, diabetes, and even cancer [2, 3]. In consequence, the quantification of BPA is of great significance. Hitherto, various approaches including spectrophotometry [4], chromatography [5], fluorescence [6] and electrochemical measurements [7] have been developed for this purpose. Among them, the voltammetric method possesses many advantages over the other methods, such as high sensitivity, good selectivity, rapid response and convenient to operate. Materials such as nanoparticles [8], carbon nanomaterials [9, 10], polymers [11] and nanocomposite [12] have been developed to fabricate electrochemical sensors to improve the detecting performance of BPA. However, novel materials with high electrocatalytic activity and low cost for BPA determination are still needed. As known, magnesium oxide (MgO) as an alkaline

earth metal oxide, has been used in electrochemical sensing of glucose [13], H_2O_2 [14], ascorbic acid, dopamine and uric acid [15] due to its biocompatability, large surface area, the capability to perform electrocatalysis and readily available. The combination of MgO with a conductive material as nanotubes and ionic liquid can further improve the sensitivity of MgO based sensors [16]. Besides, the conducting polymer known as PEDOT:PSS consists of poly(3,4-ethylenedioxythiophene) (PEDOT) and poly(4-styrene sulfonate) (PSS). PEDOT:PSS film can provide good stability and conductivity in the development of electrochemical sensors. Even though PEDOT:PSS has been combined with meldola blue, reduced graphene oxide, and graphene for electrochemical sensing of H_2O_2 [17], piroxicam, nimesulide [18], and biochemicals [19], PEDOT:PSS and MgO composites based electrochemical sensor has not been reported.

Therefore, in the present work, MgO and PEDOT:PSS (PP) were employed to fabricate a novel MgO-PP modified carbon paste electrode (MgO-PP/CPE) for the sensing of BPA. The high surface area of MgO and good conductivity of PEDOT:PSS greatly improved the sensing property of BPA. The fabricated sensor was further applied to the quantification of BPA in actual samples with satisfactory results.

2. EXPERIMENTAL

2.1. Materials

Bisphenol A, PEDOT:PSS water solution (1.5 % *w*/*w*), graphite powder (spectral reagent), paraffin oil, magnesium oxide (MgO), potassium hexacyanoferrate ($K_3[Fe(CN)_6]$), phosphoric acid (H_3PO_4, 85%), sodium hydroxide (NaOH), sodium dihydrogen phosphate (NaH_2PO_4), calcium chloride ($CaCl_2$), magnesium chloride ($MgCl_2$), aluminium chloride ($AlCl_3$), zinc acetate ($ZnAc_2$), copper sulphate ($CuSO_4$), ammonium nitrate (NH_4NO_3), absolute ethanol, glucose and phenol were purchased from Aladdin Chemical Reagents Co., Ltd.. All the chemicals used were of analytical-reagent grade. Twice-distilled water was used throughout the experiments.

2.2. Apparatus

Electrochemical measurements were carried out on CHI 650C electrochemical workstation (Chenhua Instrument, Shanghai, China). A conventional three-electrode system including a homemade MgO-PEDOT:PSS/CPE working electrode, a saturated calomel reference electrode (SCE), and a platinum wire counter electrode were employed. All the potentials quoted in the present work were referred to SCE. Chronocoulometry measurements were recorded in the potential range of 0 to 0.5 V with a pulse width of 0.25 s. Electrochemical impedance spectroscopy (EIS) measurements were performed in the frequency range of 100 kHz to 0.1 Hz with an amplitude of 0.005 V. Scanning electron microscopy (SEM) characterization was conducted on an EM-30 Plus microscope (COXEM, South Korea). All experiments were carried out at room temperature.

2.3. Electrode preparation

CPE was prepared by mixing graphite powder and paraffin oil in a ratio of 5:2 (w/w) in a beaker [20]. A portion of the resulting paste was packed firmly into the cavity (3.0 mm diameter) of a plastic tube. The electric contact was established via a copper wire. The surface of the electrode was smoothed on a weighing paper and rinsed with water. The modifier was prepared by sonicating the dispersion of 1.0 mg of MgO and 10.0 μL PEDOT:PSS in 1.0 mL water for 20 min until a homogeneous suspension was formed. Then 6.0 μL of MgO-PEDOT:PSS suspension was drop-casted directly on the surface of CPE and dried by an infrared lamp to get the modified electrode as MgO-PP/CPE. MgO/CPE and PP/CPE were prepared using the same method by drop-casting 6.0 μL of MgO suspension (1 mg mL^{-1} in water) and PEDOT:PSS aqueous solution (0.015 %, *w*/*w*) on the surface of CPE, respectively.

3. RESULTS AND DISCUSSION

3.1 Characterization of MgO-PP/CPE

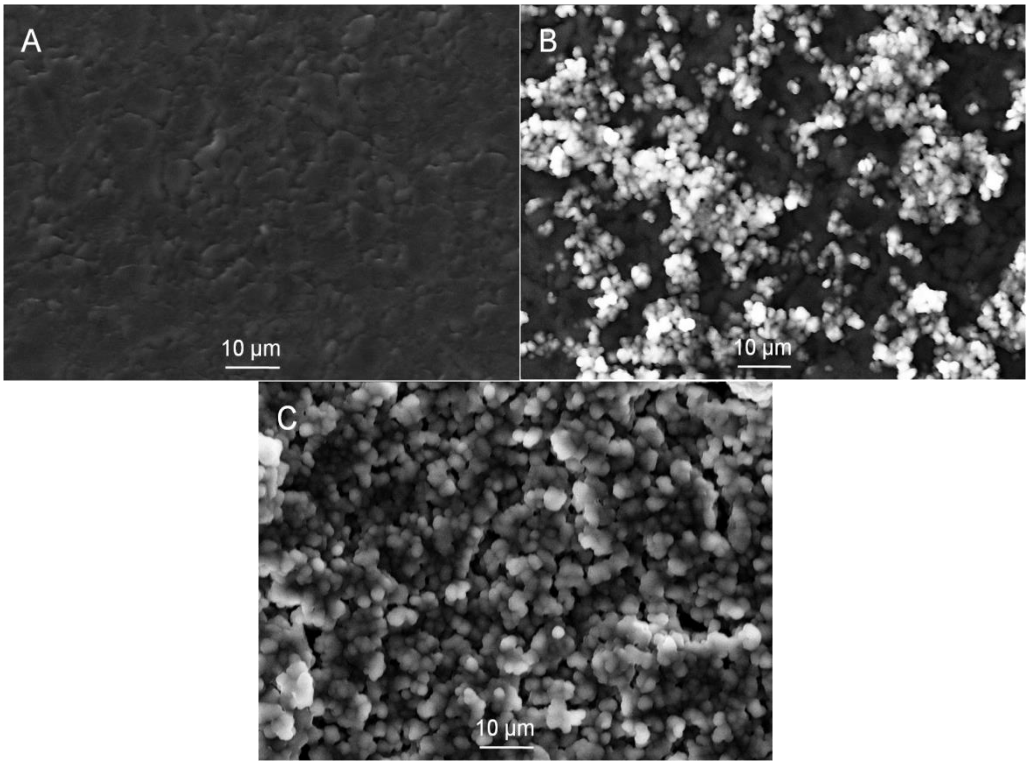

Figure 1. SEM images of (A) CPE, (B) MgO/CPE and (C) MgO-PP/CPE

The morphology of working electrodes was characterized by SEM. Fig.1 shows the SEM images of CPE, MgO/CPE, and MgO-PP/CPE, respectively. Compared with bare CPE (Fig. 1A), MgO particles are partially aggregated on the electrode surface (Fig. 1B), while MgO-PP composites are uniformly distributed on the surface of CPE (Fig. 1C). The larger size of MgO-PP particles compared to that of MgO is the result of the combination of MgO and PP. The well-distributed MgO-PP can obtain better

electrochemical properties and high stability of the sensors [18].

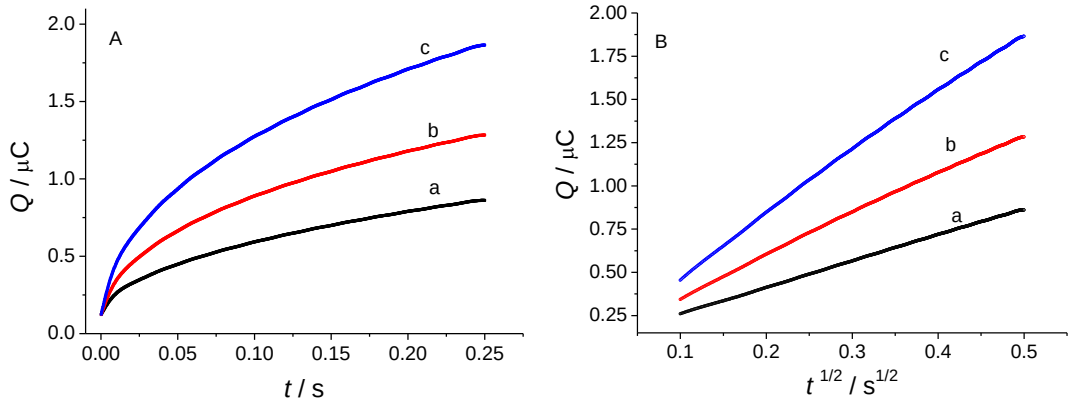

Figure 2. (A) Plots of (A) Q–t curves, and (B) Q–$t^{1/2}$ curves in 1.0 M KCl containing 0.1 mM $K_3[Fe(CN)_6]$ using (a) CPE (b) MgO/CPE, and (c) MgO-PP/CPE as the working electrode.

The electrochemically active surface areas of the working electrodes were determined by chronocoulometry based on the equation (1) given by Anson [21]:

$$Q\,(t) = (\,2nFAcD^{1/2}t^{1/2}\,) / \pi^{1/2} + Q_{dl} + Q_{ads} \quad (1)$$

where n is the electron transfer number, A is the active surface area of the working electrode, c is the concentration of substrate, D is the diffusion coefficient. Other symbols have their common meanings.

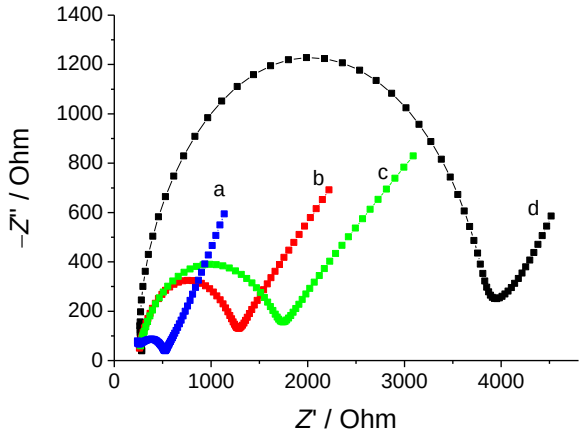

Figure 3. Nyquist plots of EIS of (a) PP/CPE, (b) MgO-PP/CPE, (c) MgO/CPE, and (d) CPE in 0.1 M KCl solution containing 5.0 mM $K_3[Fe(CN)_6]$. Frequency range: 100 kHz – 0.1 Hz. Amplitude: 0.005 V.

Fig. 2 shows the plots of $Q - t$ and $Q - t^{1/2}$ of CPE, MgO/CPE, and MgO-PP/CPE with the same geometric surface area in 1.0 M KCl containing 0.1 mM $K_3[Fe(CN)_6]$. The linear regression equations of the total charge Q of $K_3[Fe(CN)_6]$ with the square root of time $t^{1/2}$ are $Q / \mu C = 0.152 + 3.49\ t^{1/2} / s^{1/2}$ (r = 0.999) for MgO–PP/CPE, $Q / \mu C = 0.141 + 2.33\ t^{1/2} / s^{1/2}$ (r = 0.999) for MgO/CPE, and $Q / \mu C$

= 0.109 + 1.52 $t^{1/2}$ / $s^{1/2}$ (r = 0.999) for CPE, respectively. Based on the slope of the linear relationship between Q and $t^{1/2}$, the active surface area of MgO-PP/CPE and MgO/CPE is 2.3, and 1.5 times that of CPE, respectively. This increase in the active surface area is due to the high surface area of MgO and well-distributed of MgO–PP composite [16,18], which can enhance the adsorption amount of BPA, leading to better electrochemical signals [10,15].

Furthermore, the electronic transfer properties of the electrodes were investigated by EIS. As shown in Fig. 3, the semicircular part at higher frequencies indicates an electron transfer-limited process, where the diameter of the semicircular part equals the electron transfer resistance (R_{ct}), which control the electron transfer kinetics of the redox probe at the electrode interface. In this case, the diameter value of the impedance arcs follows the trend of PP/CPE < MgO-PP/CPE < MgO/CPE < CPE, indicating that the R_{ct} value of MgO-PP/CPE is smaller than that of MgO/CPE and CPE. These results suggest that the introduction of conductive polymer PEDOE:PSS to MgO accelerate the electron transfer between the analytes and electrode surface, which is beneficial for sensing. [15, 16, 19].

3.2 Electrochemical behavior of BPA on MgO-PP/CPE

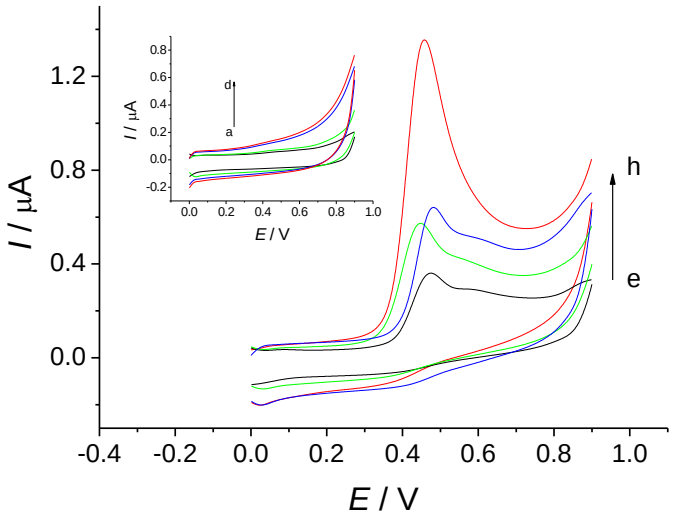

Figure 4. Cyclic voltammograms of (a, e) CPE, (b, f) MgO/CPE , (c, g) PP/CPE, and (d, h) MgO-PP/CPE in the absence (a to d, inset) and the presence (e to h) of 5.0 μM BPA in 0.1 M PBS (pH=7.0) solution at the scan rate of 100 mV s^{-1}.

The voltammetric behaviours of CPE, MgO/CPE, PP/CPE, and MgO-PP/CPE in the absence and the presence of 5.0 μM BPA in 0.1 M PBS (pH 7.0) buffer are shown in Fig. 4. As shown, a well-defined oxidation peak at 0.475 V with a peak current of 1.246 μA was observed on the anodic potential scan. On the reverse scan, no corresponding reduction peak was detected, indicating that the oxidation of BPA is an irreversible process. Under identical experimental conditions, the oxidation peak current of BPA at CPE, MgO/CPE, and PP/CPE is 0.3209 μA, 0.5033 μA, and 0.5318 μA, respectively, much lower than that at MgO-PP/CPE. These results indicate that MgO and PEDOT:PSS composite improves

the electrochemical oxidation of BPA. The enhanced electrochemical signal is due to the high surface area and optimal conductivity of MgO and PEDOT:PSS.

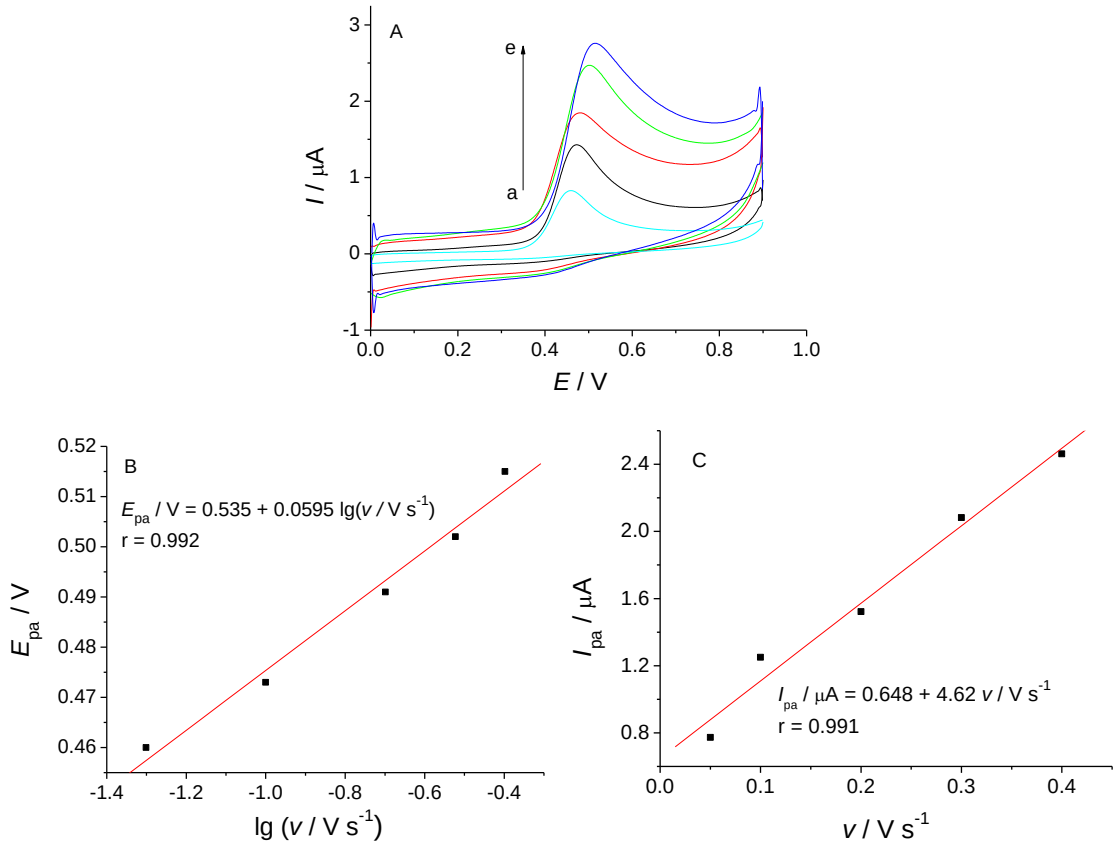

Figure 5. (A) Cyclic voltammograms of MgO-PP/CPE in 0.1 M PBS (pH=7.0) solution containing 5.0 μM BPA at various scan rates (from a to g): 0.05, 0.1, 0.2, 0.3, 0.4 V s^{-1}. (B) Plot of E_{pa} vs. lg*v*. (C) Plot of I_{pa} vs. *v*.

To understand the reaction process of BPA on the proposed sensor, the influence of scan rate *v* on the response of BPA at MgO-PP/CPE was investigated by CV (Fig. 5A). As shown, the peak potential E_p is proportional to the logarithm of *v* (Fig. 5B). The peak current I_{pa} increases with the increase of *v* and is proportional to *v* from 50 to 400 mV s^{-1} (Fig. 5C), which indicates an adsorption confined redox process. As for an adsorption-controlled irreversible electrode process, E_{pa} follows the following equation [22]:

$$E_{pa} = E^{o} + (\frac{RT}{\alpha nF})\ln(\frac{RTk^{o}}{\alpha nF}) + (\frac{RT}{\alpha nF})\ln v \quad (2)$$

Where α is the transfer coefficient, *n* is the electron transfer number involved in the rate-determining step, *v* is the scan rate, other symbols have their common meanings. According to the slope of Fig. 5B, the value of αn is calculated to be 1.01. Given that α is 0.5 for an irreversible electrochemical process, the number of the transferred electron (*n*) for the electrochemical oxidation of BPA is 2.

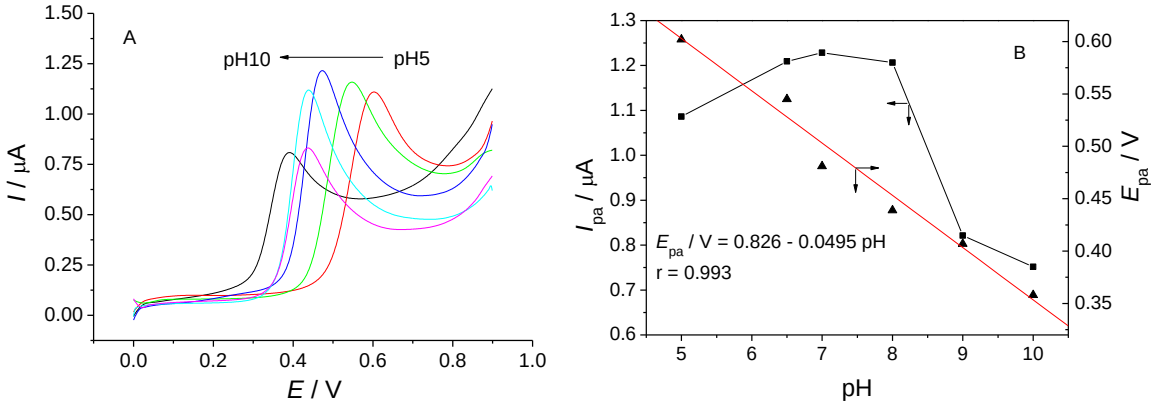

Figure 6. (A) Linear sweep voltammograms of MgO-PP/CPE in 0.1 M PBS buffer with various pH values. Scan rate: 100 mV s^{-1}. (B) plots of I_{pa}, and E_{pa} vs. pH.

Moreover, the peak potential of BPA oxidation shows a negative shift upon the increase of pH, indicating a proton dissociation process during BPA oxidation (Fig. 6). The relationship between the peak potential and pH value follows the equation of E_{pa} / V = 0.826 − 0.0495 pH (r = 0.993). The slope of 49.5 mV/pH suggests that the number of the electron and the proton involved in the electrochemical oxidation of BPA are equal. Thus, the electrochemical oxidation of BPA at MgO-PP/CPE can be described as a 2-electron and 2-proton process shown below:

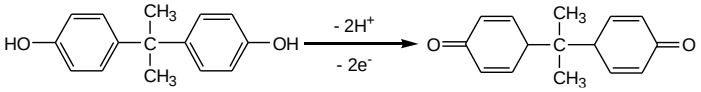

3.3 Optimization of parameters

3.3.1 MgO and PP content and loading amount in MgO-PP/CPE

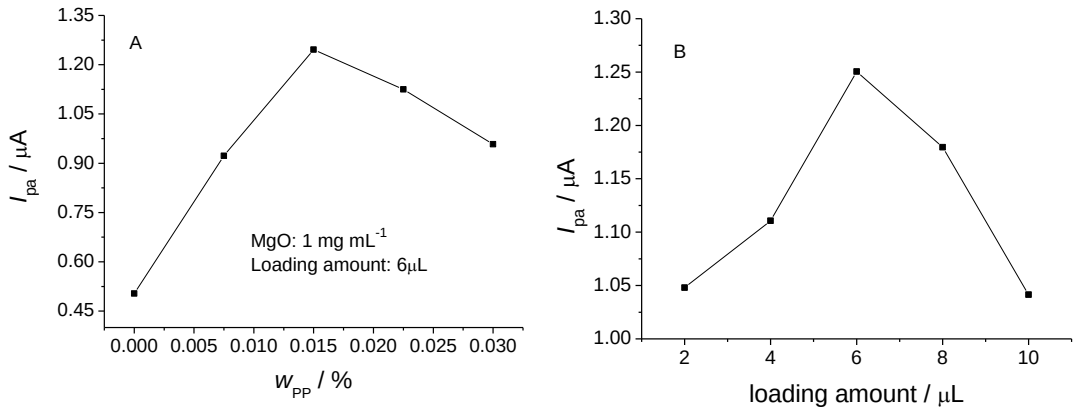

Figure 7. Plots of (A) I_{pa} vs. w_{PP} in MgO-PP composite, and (B) I_{pa} vs. loading amount of MgO-PP. I_{pa} is the electrochemical oxidation peak current of BPA in 0.1 M PBS (pH=7.0) containing 5.0 μM BPA.

To get the optimum responses of MgO-PP/CPE to the electrochemical oxidation of BPA, the effects of PP content w_{PP} in MgO-PP composite and loading amount of MgO-PP (1mg MgO + 1mL 0.015% PP) on the peak current I_{pa} of the electrochemical oxidation of BPA were investigated. As shown in Fig. 6, the I_{pa} plateau is at the PP content of 0.015% (Fig. 6A) and the MgO-PP loading of 6 μL (Fig. 6B). In consequence, 6 μL of MgO-PP (1mg MgO + 1mL 0.015% PP) is the optimum condition for the preparation of MgO-PP/CPE.

3.3.2 pH

The voltammetric responses of 5.0 μM BPA at the MgO-PP/CPE in sodium acetate–acetic acid, ammonia–ammonium chloride, Britton-Robinson and phosphate buffer (PBS) were examined. It was observed that the oxidation peak of PBA is more well-defined and more sensitive in the PBS buffer than in other solutions. The influence of solution pH values (from 5.0 to 10.0) on the response of BPA at MgO-PP/CPE was investigated by LSV in PBS buffer. As shown in Fig. 6, the oxidation peak currents of BPA increase with the increase of the pH value when pH value is below 6.5, and reach the maximum value among pH 6.5 to pH 8. When pH value is above 8, the peak currents begin to decrease. Thus, 0.1 M PBS buffer (pH=7.0) is chosen as the supporting electrolyte, which is optimal for the adsorption and electrochemical oxidation of BPA.

3.3.3 Accumulation potential and accumulation time

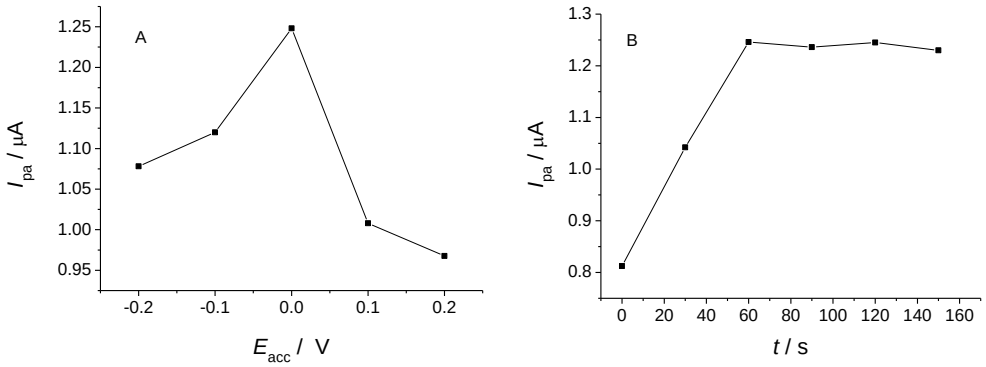

Figure 8. Plots of (A) I_{pa} vs. accumulation potential (E_{acc}), and (B) I_{pa} vs. accumulation time (t_{acc}). I_{pa} is the oxidation peak current of BPA at MgO-PP/CPE.

The influences of accumulation potential and accumulation time on the oxidation peak current of BPA at MgO-PP/CPE were also investigated (Fig. 8). When the accumulation potential changes from − 0.2 to 0.2 V, the oxidation peak current of BPA peaks at 0 V (Fig. 8A). The peak current increases significantly within the first 60 s of accumulation and then level off (Fig. 8B). Thus, an open-circuit accumulation of 60 s is applied in the quantification of BPA.

3.4 Calibration curve and detection limit

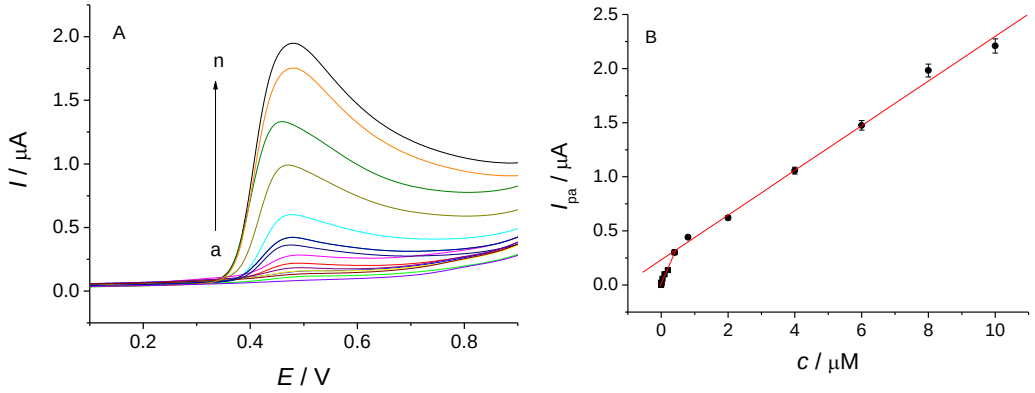

Figure 9. (A) Linear sweep voltammograms of BPA in 0.1 M PBS (pH=7.0) solution. The concentration of BPA for a to n are: 0, 0.001, 0.005, 0.01, 0.05, 0.1, 0.2, 0.4, 0.8, 2, 4, 6, 8, 10 μM. (B) Plot of I_{pa} vs. BPA concentration.

Fig. 9 shows the linear sweep voltammograms (LSV) of BPA at MgO-PP/CPE under optimized experimental conditions. As shown, the response current increases with the increase of BPA concentration, and is linear with BPA concentration in the range of 0.001 to 10 μM. Two linear ranges were observed. The linear regression equations are I / μA = 0.01857 + 0.6931 c / μM (c = 0.001 ~ 0.4 μM, r = 0.9946), and I / μA = 0.2448 + 0.2045 c / μM (c = 0.4 ~ 10 μM, r = 0.9971), respectively. The detection limit is 0.5 nM (3S/N). Table 1 displays a comparison of the analytical characteristics of the present work with the previous reports. The improved performance of MgO-PP/CPE for BPA electrochemical oxidation can be attributed to the large surface area of MgO and the facile electron transfer properties of PEDOT:PSS.

Table 1. Comparison of analytical characteristics of various sensors for BPA

Sensors	Linear Range (μM)	Detection Limit (nM)	Sensitivity (μM mM^{-1})	Reference
PAMAM–Fe_3O_4/GCE	0.01 – 3.07	5	–	23
NiO/CNT/IL/CPE	0.08 – 500	40	0.2294	24
Cu_2O-rGO/GCE	0.1 – 80	53	3.504	25
CTAB/Ce-MOF/GCE	0.005 – 5 – 50	2	0.802, 0.092	26
CNT-OH/GCE	0.004 – 0.105	3.5	8.812	9
rGO/ABPE	0.008-0.01-100	0.6	5142, 810, 171	10
CNT/TiO_2/CPE	0.1– 60	56	2.9	27
PEDOT-il/SPCE	0.1 – 500	20	226.1	11
La^{3+}-Co_3O_4/SPCE	0.5– 900	61	33.8	28
GN/GCE	0.1– 100	35	460	29
NP-PtFe/GCE	0.2 – 96	170	64	30
MgO-PEDOT:PSS/CPE	0.001– 0.4 – 10	0.5	693.1, 204.5	Present Work

PAMAM, polyamidoamine dendrimer; IL, ion liquid; rGO, reduced graphene oxide; CTAB/Ce-MOF, cetyltrimethylammonium bromide/Ce-metal organic framework; CNT-OH, hydroxylated multi-walled carbon nanotubes; ABPE, acetylene black paste electrode; SPCE, screen-printed carbon electrodes; La^{3+}-Co_3O_4, La^{3+} doped Co_3O_4 nanocube; GN, graphite nanoparticle; NP-PtFe, nanoporous PtFe alloy.

3.5 Repeatability, reproducibility, stability and interference

The repeatability, reproducibility and stability of MgO-PP/CPE were studied. The relative standard deviation (RSD) for seven replicate measurements of 5.0 μM BPA at MgO-PP/CPE is 3.95 %. The RSD of six pieces of MgO-PP/CPE with the same surface area for the individual quantification of 5.0 μM BPA is 3.86 %. The stability of the modified electrode was tested after stored under the dry condition for 15 days at room temperature and the current responses maintain 95.6 % of the original value. These results demonstrate the good repeatability, reproducibility and stability of the sensor.

The influence of some common interferences on the quantification of BPA was also tested. The tolerable limit is defined as the concentration of possible interfering species, which gives a relative error of less than ± 5.0 % in the quantification of 5.0 μM BPA. The results show that 100-fold of Ca^{2+}, Mg^{2+}, Al^{3+}, Zn^{2+}, Cu^{2+}, NH_4^+, Cl^-, Ac^-, NO_3^-, SO_4^{2-}, ethanol, glucose, and phenol do not interfere with the quantification, proving that the selectivity of the proposed method is acceptable.

3.6 Practical applications

The potential application of the proposed method was evaluated by monitoring the concentration of BPA in water samples. Standard addition method was used for the analysis. As seen in Table 2, the recoveries are in the range of 95.2 % to 104 %, suggesting that the MgO-PP/CPE is promising for detecting BPA in the real samples.

Table 2. Results of quantification of BPA in water samples

Sample	BPA added (μM)	BPA found (μM)*	Recovery (%)
Tap water	0	_	_
	0.10	0.103	103
	0.50	0.476	95.2
	2.50	2.438	97.5
Plastic bottle water	0	_	_
	0.10	0.104	104
	0.50	0.493	98.6
	2.50	2.530	101

* Mean value of five measurements.

4. CONCLUSIONS

A novel modified electrode was fabricated based on MgO and conductive polymer PEDOT:PSS composite modified carbon paste electrode. The modified electrode improves the electrochemical activity of bisphenol A due to the high surface area of MgO and the excellent electron transfer efficiency of conductive polymer PEDOT:PSS. The designed sensor for bisphenol A measurement possesses a wide linear range, high sensitivity, low detection limit, good selectivity, and stability.

ACKNOWLEDGEMENTS
The authors would like to acknowledge financial support from the National Natural Science Foundation of China (Grant No.21675123) and the Science & Technology Innovation Foundation of Xi'an Shiyou University (No. Z09137).

References

1. N. Salgueiro-González, S. Muniategui-Lorenzo, P. López-Mahía, D. Prada Rodríguez, *Anal. Chim. Acta,* 962 (2017) 1.
2. J.R. Rochester*, Reprod. Toxicol*., 42 (2013) 132.
3. J. Michałowicz, *Environ.Toxicol. Pharm.,* 37 (2014) 738.
4. N.K. Temel, R. Gürkan, *Anal. Methods,* 9 (2017) 1190.
5. S. Li, Y. Jin, H. Zhao, Y. Jiang, Z. Cai, *Chemosphere,* 222 (2019) 235.
6. K.E. McCracken, T. Tat, V. Paz, J.Y.Yoon, *RSC Adv.,* 7 (2017) 9237.
7. K. Varmira, M. Saed-Mocheshi, A.R. Jalalvand*, Sens. Bio-Sens. Res.,* 15 (2017) 17.
8. Y. Zhang, Y. Cheng, Y. Zhou, B. Li, W. Gu, X. Shi, Y. Xian, *Talanta,* 107 (2013) 211.
9. M.S. Cosioa, A. Pellicanò, B. Brunetti, C.A. Fuenmayor, *Sens. Actuators B,* 246 (2017) 673.
10. P. Deng, Z. Xu, Y. Kuang, *J. Electroanal. Chem.,* 707 (2013) 7.
11. J.Y. Wang, Y.L. Su, B.H. Wu, S.H. Cheng*, Talanta,* 147(2016)103.
12. K.J. Huang, Y.J. Liu, Y.M. Liu, L.L. Wang, *J. Hazard. Mater.,* 276 (2014) 207.**J**
13. A. Umar, M.M. Rahman, Y.B. Hahn, *Electrochem. Commun.,* 11 (2009) 1353.
14. X. Dong, M. Li, N. Feng, Y. Sun, C. Yang Z. Xu, *RSC Adv.,* 5 (2015) 86485.
15. M. Li, W. Guo, H. Li, W. Dai, B. Yang, *Sens. Actuators B,* 204 (2014) 629.
16. M. Abbasghorbani, *Int. J. Electrochem. Sci.,* 12 (2017) 11656.
17. H.W. Siao, S.M. Chen, K.C. Lin, *J. Solid State Electrochem.,* 15 (2011) 1121.
18. A. Wong, A.M. Santos, O. Fatibello-Filho*, J. Electroanal. Chem.,* 799 (2017) 547.
19. C. Sriprachuabwong, C. Karuwan, A. Wisitsorrat, D. Phokharatkul, T. Lomas, P. Sritongkham, A. Tuantranont, *J. Mater. Chem.,* 22 (2012) 5478.
20. X. Tian, J. Song, *Chin. J. Anal. Chem.,* 34 (2006) 1283.
21. F. Anson, *Anal. Chem.,* 36 (1964) 932.
22. E. Laviron, *J. Electroanal. Chem. Interfacial Electrochem.,* 52 (1974) 355.
23. H. Yin, L. Cui, Q. Chen, W. Shi, S. Ai, L. Zhu, L. Lu, *Food Chem.,* 125 (2011) 1097.
24. B. Nikahd, M.A. Khalilzadeh, *J. Mol. Liq.,* 215 (2016) 253.
25. R.G. Shi, J. Liang, Z.S. Zhao, A.F. Liu, Y. Tian, *Talanta,* 169 (2017) 37.
26. Jing Zhang, Xiaojian Xu, Lu Chen, *Sens. Actuators B,* 261 (2018) 425.
27. H. Ezoji, M. Rahimnejad, *Sens. Actuators B,* 274 (2018) 370.
28. H Beitollahi, H Mahmoudi Moghaddam, S Tajik, *Anal. Lett.,* 52(2019)1432.

29. Dong X, Qi X, Liu N, Yang Y, Piao Y, *Sensors*, 17 (2017) 836.
30. Tian C, Chen D, Nali Lu, Li Y, Cui R, Han Z, Zhang G, *J. Electroanal. Chem.*, 830-831 (2018) 27.